*Progress In Electromagnetics Research Letters, Vol. 43, 83–94, 2013*

# INTEGRATED METAL-INSULATOR-METAL PLASMONIC NANO RESONATOR: AN ANALYTICAL APPROACH

**Rehab Kotb[1, 2], Yehea Ismail[2], and Mohamed A. Swillam[3, *]**

[1]The Nanotechnology Program at The American University in Cairo (AUC), Egypt

[2]The Center for Nanoelectronics and Devices (CND), The American University in Cairo/Zewail City of Science and Technology, Cairo, Egypt

[3]The Department of Physics and Yousef Jameel Science and Technology Research Center (YJ-STRC), School of Science and Engineering, The American University in Cairo, Egypt

**Abstract**—A novel structure is proposed as an inline resonator. The resonator has low loss, compact size and good sensing characteristics. A simple analytical form to the plasmonic waveguide discontinuity, filter resonance response and cascaded filters behavior is proposed. The model is extracted from the waveguide physical parameters and provides a physical insight into the structure of the filter. This model is simple, accurate, and shows a good agreement with FDTD simulations. The ability of the model to provide a good methodology to obtain high quality filters using cascaded inline filtering is verified using FDTD. The proposed nanofilter can be used in various plasmonic applications such as sensing, biomedical diagnostics and on-chip interconnects. Using cascaded filters, a higher quality filter is achieved.

## 1. INTRODUCTION

Guiding light on a sub-wavelength scale using plasmonic waveguides has empowered many nanophotonic applications. Nanoscale plasmonic waveguides utilize surface plasmon polaritons (SPPs) to enhance field strength near the metal-dielectric interface. SPP waveguides can be

*Received 15 July 2013, Accepted 13 August 2013, Scheduled 9 October 2013*

* Corresponding author: Mohamed A. Swillam (m.swillam@aucegypt.edu).

used in sensing, biomedical diagnostics, and surface enhanced Raman Scattering applications [1–3]. The scale mismatch between nanoscale electronics and microscale optical devices can be solved using SPP waveguides with their ability to confine light at a subwavelength scale. As a result, they can be also used as high bandwidth optical interconnects for on-chip applications [4].

Among various configurations, The Metal-Insulator-Metal (MIM) structure is considered as a suitable candidate for the aforementioned applications. Plasmonic waveguides consist of a sub-wavelength dielectric core surrounded by metal cladding. A high density integration of plasmonic devices can be achieved by reducing the core width to a few tens of nanometers.

This configuration, however, suffers from high propagation losses which allow only for a few wavelengths length of the structure. Due to its ultra small core size, the coupling to and from this core is challenging. Recently, this coupling dilemma has been resolved by introducing a novel non-resonant coupling mechanism to and from the conventional silicon waveguide and the plasmonics slot waveguide (PSW); a 3D version of this MIM configuration has been proposed [5, 6]. On the other hand, in order to avoid the propagation loss impact on the performance of the plasmonic devices, the device length has to be in the order of a few microns only. This challenge has also been satisfied in various new functional designs [7, 8].

Wavelength filtering and sensing functions are needed for most plasmonic applications. Recently, different designs to get a filtering response have been proposed [7–12]. Most of these designs are mainly based on resonance effect and show band rejection (notch) filter response. Band transmission response is considered as an important filter response especially for wavelength division multiple (WDM) access optical systems and for sensing applications. Thus, novel plasmonic filter designs for band transmission filters are of prime importance.

In addition, numerical techniques are commonly used to analyze the performance of the plasmonic structures. In particular, Finite Difference Time Domain (FDTD) simulation is the conventional numerical method for this purpose. However, this technique doesn't give the designer a detailed physical insight into the design of the device. In addition, it requires long simulation time and tremendous computational resources.

Thus, there is a real need for an effective tool that allows for understanding the behavior of the surface plasmon wave inside the various structures and to be able to accurately predict the response.

In this paper, we propose a novel structure as an inline plasmonic

resonance-based filter with good quality factor and minimum insertion loss. We also introduce an analysis for this structure using a closed form model that serves as a good design tool for a cascaded version of this resonator. The cascaded filter has sharp response which is useful in sensing applications. This closed form model is utilized to describe a plasmonic wavelength selective filter. FDTD simulations are used to confirm the accuracy of this model. This FDTD has been recently proved to show good match with the experimental measurements [5, 6]. Thus, the good match between our model and the FDTD suggests a good match with the experimental results. The experimental verification of the model will be discussed in future publications.

Highly efficient, optimized, various filter designs can be achieved using this model. The model is simple and straightforward. This filter can also be utilized as an integrated optical modulator.

We start by presenting the theoretical analysis of the plasmonic waveguide discontinuity in Section 2. The closed form model is proposed to describe the behavior of a resonant filter in Section 3. In Section 4, a high quality cascaded resonant filter design is proposed using our model. The sensing applications of this filter are discussed in Section 5. Finally, the conclusion is given in Section 6.

## 2. THEORETICAL ANALYSIS TO THE PLASMONIC WAVEGUIDE DISCONTINUITY

The inline filter, shown in Fig. 1, is a simple Fabry-Perot based plasmonic resonator. In order to develop a closed form model that describes the behavior of this resonator, the waveguide discontinuity

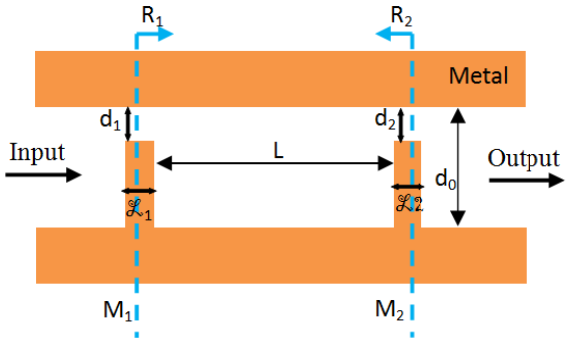


**Figure 1.** Schematic diagram of the plasmonic inline resonator.

needs to be investigated and analyzed first. Thus, we initially develop an analytical model for the waveguide discontinuity shown in the inset of Fig. 2.

A quasistatic approximation can be applied on Metal-Insulator-Metal (MIM) waveguides as long as the dielectric core width is much smaller than the plasmonic wavelength ($d < \lambda_{\text{spp}}/6$) [7]. In this approximation, the plasmonic waveguide junctions can be accurately represented by the impedance model [8, 13]. Hence, the waveguide discontinuity shown in Fig. 2 can be considered as three cascaded waveguides, each having a characteristic impedance ($Z = V/I$). The impedance of the TM mode in the plasmonic waveguide can be calculated using [13]

$$Z = \frac{V}{I} = \frac{\beta_{\text{MIM}} d}{\omega \varepsilon} \tag{1}$$

where $\beta_{\text{MIM}}$ is the MIM propagation constant, $d$ the width of the dielectric core, and $\omega$ the angular frequency. Despite the fact that the SPP modes are confined to the metal-dielectric interface, the propagation modes in MIM structure are created as a result of the coupling between the interfaces' modes. Those coupled modes appear when the separation between the interfaces is less than the decay length of the interface mode. By solving Maxwell equations in the TM case, we can get the wave equation of the propagating waves. To be specific, the coupled modes are localized at the metal-dielectric interface and to achieve the field continuity that fulfill the wave equation, the propagation constant ($\beta$) has to follow the form [14]

$$k_i^2 = \beta^2 - k_0^2 \varepsilon_i \tag{2}$$

where $k_i$ is the transverse component of the wave vector at the first and second interface or at the interface "$i$". Therefore, the dispersion relation of the odd modes is expressed by

$$\tanh k_1 d = -\frac{k_2 \varepsilon_1}{k_1 \varepsilon_2} \tag{3}$$

As a matter of fact, the fundamental odd mode is the most interesting mode from the energy confinement point of view. By solving the Equations (2) and (3), the properties of the coupled propagating modes can be investigated.

This propagation constant is essential to calculate the waveguide impedance in (1). This waveguide impedance is utilized to estimate the reflection and transmission power at each junction discontinuity. For example a waveguide discontinuity as the one shown in Fig. 2, the propagating wave suffers from partial reflection. The net reflection of

this discontinuity can be calculated by taking into consideration the multiple reflections between the first and second interfaces [7, 8, 15]

$$R = \Gamma_0 + \frac{T_0 T_1 \Gamma_2 e^{-2\varphi}}{1 - \Gamma_1 \Gamma_2 e^{-2\varphi}} \tag{4}$$

where $\Gamma_i$ is the elementary reflection coefficient, and $T_i$ is the transmittance coefficient.

$$\Gamma i = \frac{Z_{i+1} - Z_i}{Z_{i+1} + Z_i} \tag{5}$$

The term $\varphi = (\alpha + j\beta)L_s$ is the phase delay between the two adjacent discontinuities, where $\alpha$ is the loss factor and $L_s$ the length of the intermediate waveguide. This reflection model has been verified and compared with FDTD simulations [16] as shown in Fig. 2. The mesh size used in the FDTD simulations is 3.0 nm, the simulation region is terminated using perfectly matched layer (PML) absorbing boundary conditions, and the model of the used silver material reported in [17]. In addition, the model is verified at different widths and at different lengths of the waveguide at a wavelength of 1550 nm. Varying the width of the waveguide ($d_1$) with respect to ($d_0$) is shown in Fig. 3. Moreover, the length of the intermediate waveguide ($L_s$) is varied from 50 nm to 100 nm when $d_0$ is 200 nm and $d_1$ is 100 nm as shown in Fig. 4.

## 3. THEORETICAL ANALYSIS OF THE PLASMONIC NANO-FILTER

Now, the resonator can be analyzed as an optical Fabry-Perot resonator where the two transverse metal sides are acting as two mirrors ($M_1$ and $M_2$). The reflection of each mirror ($R_1$ and $R_2$) is determined as explained previously using (4).

The power transmission coefficient for this structure can be modified to include the loss thusly:

$$T = \frac{(1 - R_1)(1 - R_2)}{(1 - \sqrt{R_1 R_2} e^{2\alpha L})^2 + 4\sqrt{R_1 R_2} e^{2\alpha L} \sin^2(\beta L)} \tag{6}$$

The resonator length is calculated as $L = q\lambda_0/(2n_{eff})$, $\lambda_0$ is the resonance wavelength, $q$ is an integer value and $n_{eff}$ is the effective index of the dielectric core.

By comparing this model to the FDTD simulations, good matching is obtained with an error less than 2% as shown in Fig. 5.

In this figure, we compare between the FDTD results, the model given in (6) using the reflection coefficient extracted from FDTD simulations [Model (1)], and the filter model using the reflection

coefficient model we explained previously in (4) [Model (2)]. It is worth noting that most of the recent attempts in [8–10], [18] utilize approaches similar to the one used for [Model (1)]. However, this model depends on the FDTD to attain the amount of the coupled power to the resonator. It is also clear from the comparison that the results obtained from our model, [Model (2)], have a good match with [Model (1)] and the FDTD with no need for any electromagnetic simulations.

As shown in Fig. 5, the maximum transmittance is ∼91% at 1550 nm wavelength which shows that the proposed structure as small loss that does not not exceed 9% at the peak wavelength. The figure also shows that the Full Width Half Maximum (FWHM) bandwidth is 50 nm. Fig. 6 illustrates the electric field intensity at resonance wavelength, 1550 nm in our design, and off resonance, at 1800 nm. Using this model, the transmission function can be optimized by properly choosing the filter parameters, such as the dimensions of the filter and the dielectric inside the core.

## 4. CASCADED FILTERS

Cascading filters are a commonly used method to get sharper resonance and narrow band filtering. Using this concept, we can cascade optical

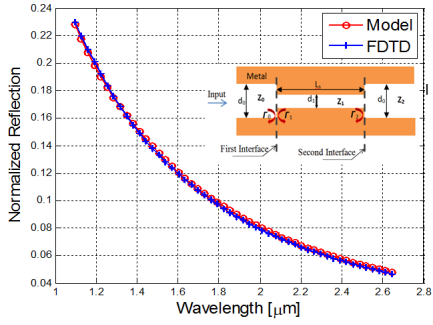


**Figure 2.** Normalized reflection obtained from FDTD simulation and the reflection coefficient given in (4) as a function of the wavelength. The used dimensions of the waveguide structure shown in the inset of Fig. 2 are $d_0 = 200$ nm, $d_1 = 100$ nm, and $L_s = 90$ nm.

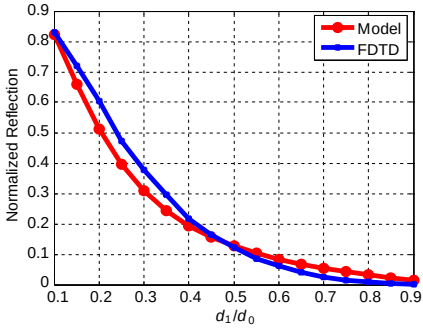


**Figure 3.** Normalized reflection obtained using FDTD simulation and the reflection coefficient given in (4) as a function of the waveguide width. The length of the intermediate waveguide $L_s = 90$ nm.

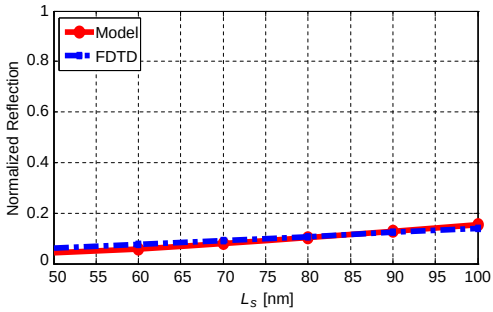


**Figure 4.** Normalized reflection obtained from FDTD simulation and the reflection coefficient given in (4) as a function of the waveguide length ($L_s$). The width of the waveguide $d_0 = 200\,\text{nm}$ and $d_1 = 100\,\text{nm}$.

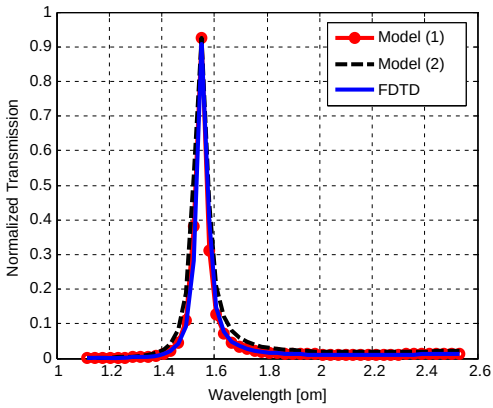


**Figure 5.** Normalized transmission obtained from FDTD simulation and the power transmission coefficient given in (6) as a function of the wavelength. The used dimensions of the filter shown in Fig. 1 are $d_0 = 250\,\text{nm}$, $d_1 = 20\,\text{nm}$, $d_2 = 30\,\text{nm}$, $L_1 = L_2 = 90\,\text{nm}$, $L = 734\,\text{nm}$.

filters as shown in Fig. 7 to get a sharper response.

As can be shown in Fig. 7, the wave emerging from the first stage of the cascaded filters propagates a distance $L_i$ before entering the second stage. It has to be taken into consideration that the propagating wave from the first to the second filter suffers from multiple reflections between the two filters. Therefore, the propagation factor ($\mathbf{P}$) can be described as:

$$\mathbf{P} = \frac{e^{-(\alpha+j\beta)L_i}}{1 - R_1 R_2 e^{-2(\alpha+j\beta)L_i}} \tag{7}$$

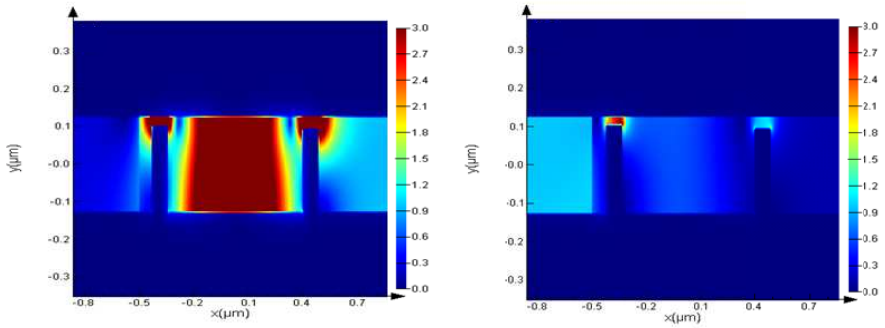


**Figure 6.** Electric field intensity (a) at resonance frequency 1550 nm, (b) off resonance at 1800 nm.

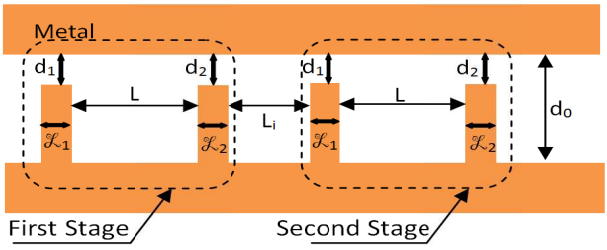


**Figure 7.** Schematic diagram of two cascaded filters.

As a consequence, the total transmission ($T_f$) of the multistage filter shown in Fig. 7 can be calculated using the formula:

$$T_f = T_1 \mathbf{P} T_2 \tag{8}$$

where $T_1$ and $T_2$ are the transmission function of the first and the second stage respectively as calculated in (6), and $\mathbf{P}$ is the propagation operator as given in (7).

In general, the distance between the two filters ($L_i$) can be considered as an intermediate cavity which has its own resonance frequency. This effect is taking into account by using the modified propagation operator $\mathbf{P}$ as given in (7).

In Fig. 8, we compare between the FDTD results, the cascaded filter model given in (8) using the reflection coefficient extracted from FDTD simulations [Model (1)], and the filter model using the reflection coefficient model we proposed in (4) [Model (2)]. Using this method, we managed to achieve a sharp resonance tunable filter with maximum

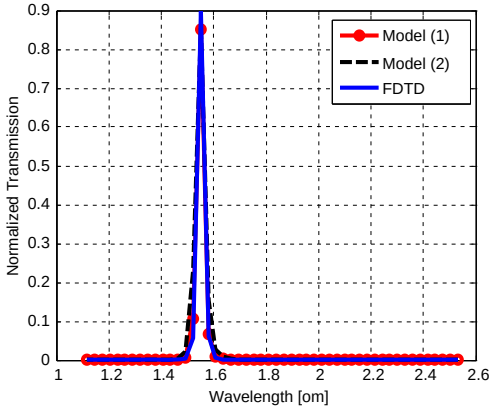


**Figure 8.** Normalized transmission of the cascaded filter ($T_f$) as a function of the wavelength. The used dimensions of the cascaded filter shown in Fig. 7 are $d_0 = 250\,\text{nm}$, $d_1 = 20\,\text{nm}$, $d_2 = 30\,\text{nm}$, $L_1 = L_2 = 90\,\text{nm}$, $L = 734\,\text{nm}$, $L_i = 330\,\text{nm}$.

transmittance ∼90% at 1550 nm wavelength and FWHM bandwidth 30 nm as shown in Fig. 8. Thus, this inline filter has small footprint, narrow FWHM, and high quality factor ∼52. Fig. 9 illustrates the electric field intensity at resonance wavelength, 1550 nm in our design, and off resonance, at 1800 nm. These configurations lend themselves for ease of the tuning mechanism that can be done electrically by including a tunable material inside the slot. They also open new directions for switching and modulation applications.

## 5. DISCUSSION

Numerous applications have been developed in the last decade depending on SPP sensing techniques. Recently, chemical, physical and biological sensors using Surface Plasmon Resonator (SPR) methodologies are receiving growing attention. Currently, most of the designs for SPR require bulky input and output peripherals [19, 20]. On the other hand, integrated plasmonic sensors have lower sensitivity but are essential for on-chip and microfluidic applications with integrated peripherals. The proposed filter can work as a highly effective integrated sensor. This filter has a relatively high sensitivity, as shown in Fig. 10. Changing the refractive index of the dielectric material by 0.1, we get 150 nm shifting in resonance wavelength and changing it by 0.01 we get 30 nm shifting in the resonance wavelength. As a result, the sensitivity of this device is ranging from 1500 nm $\text{RIU}^{-1}$ to 3000 nm

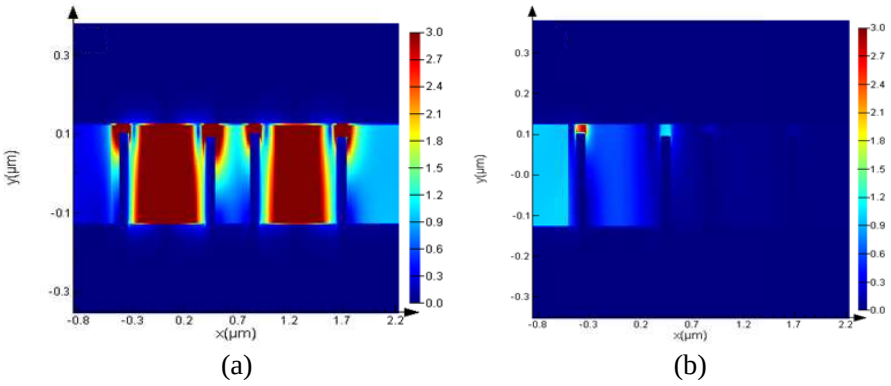


**Figure 9.** Electric field intensity (a) at resonance frequency 1550 nm, (b) off resonance at 1800 nm.

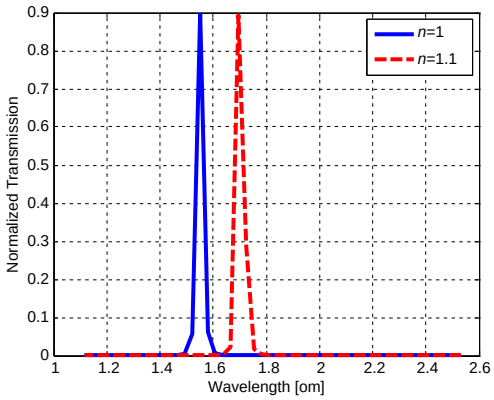


**Figure 10.** Comparison between the filter outputs when the refractive index of the dielectric material changes by 0.1.

$\mathrm{RIU}^{-1}$.

The same structure can be also utilized as an optical modulator if the core region is filled with an active material that can be controlled. The control can be electrically by applying an external electric field to change the refractive index of the active material. For such modulation scheme the core martial has to have good electro-optic effect. Such as InP or polymers. The control can also be done using thermo-optic material by heating the material to change its refractive index. Thus, the proposed structure can be utilized for various applications.

## 6. CONCLUSION

We propose an analytical model of a novel plasmonic nano filter. The plasmonic waveguide discontinuity is investigated for the first time, to the best of our knowledge, and the transmission power due to the filter cavity resonance is provided. By cascading filters, a high quality filter with sharp resonance and narrow bandwidth is obtained. This structure can also work as an integrated sensor with high sensitivity. The proposed model has good agreement with FDTD simulation results. Therefore, it helps in optimizing the design to get the required response in a short time with a low memory requirement compared to FDTD simulations. In addition, it gives the designer a physical insight into the behavior of the structure which is concealed in case of numerical simulations.

## REFERENCES

1. Berini, P., "Bulk and surface sensitivities of surface plasmon waveguides," *New J. Phys.*, Vol. 10, 105010, 2008.
2. Homola, J., "Present and future of surface plasmon resonance biosensors," *Anal. Bioanal. Chem.*, Vol. 377, 528–539, 2003.
3. Maier, S. A., "Plasmonic field enhancement and SERS in the effective mode volume picture," *Opt. Express*, Vol. 14, 1957–1964, 2006.
4. Dionne, J. A., L. A. Sweatlock, and H. A. Atwater, "Plasmonic slot waveguides: Towards chip-scale propagation with subwavelength-scale localization," *Phys. Rev. B*, Vol. 73, 035407, 2006.
5. Lau, B., M. A. Swillam, and A. S. Helmy, "Hybrid orthogonal junctions: Wideband plasmonic slot-silicon waveguide couplers," *Opt. Express*, Vol. 18, No. 26, 27048–27059, 2010.
6. Lin, C., H. K. Wang, B. Lau, M. A. Swillam, and A. S. Helmy, "Efficient broadband energy transfer via momentum matching at hybrid guided-wave junctions," *Applied Physics Letters*, Vol. 101, 123115, 2012.
7. Lin, C., M. A. Swillam, and A. S. Helmy, "Analytical model for metal-insulator-metal mesh waveguide architectures," *J. Opt. Soc. Am. B*, Vol. 29, No. 11, 3157–3169, 2012.
8. Swillam, M. A. and A. S. Helmy, "Feedback effects in plasmonic slot waveguides examined using a closed-form model," *Photon.Technol. Lett.*, Vol. 24, 497–499, 2012.
9. Yun, B., G. Hu, and Y. Cui, "Theoretical analysis of a nanoscale plasmonic filter based on a rectangular metal-insulator-metal

waveguide," *J. Phys. D, Appl. Phys.*, Vol. 43, No. 38, 385102-1–385102-8, 2010.

10. Han, Z., V. Van, W. N. Herman, and P.-T. Ho, "Aperture-coupled MIM plasmonic ring resonators with sub-diffraction modal volumes," *Opt. Express*, Vol. 17, No. 15, 12678–12684, 2009.
11. Lin, X.-S. and X.-G. Huang, "Tooth-shaped plasmonic waveguide filters with nanometeric sizes," *Opt. Lett.*, Vol. 33, 2874–2876, 2008.
12. Huang, Y., C. Min, L. Yang, and G. Veronis, "Nanoscale plasmonic devices based on metal-dielectric-metal stub resonators," *International Journal of Optics*, Vol. 2012, Article ID 372048, 13, 2012.
13. Veronis, G. and S. Fan, "Bends and splitters in metal-dielectricmetal subwavelength plasmonic waveguides," *Appl. Phys. Lett.*, Vol. 87, 131102, 2005.
14. Maier, S. A., *Plasmonics: Fundamentals and Applications*, Springer, 2007.
15. Pozar, D. M., *Microwave Engineering,* 2nd Edition, John Wiley & Sons, Toronto, 1998.
16. Lumerical, "Multicoefficient material modelling in FDTD," http://www.lumerical.com/solutions/whitepapers/fdtd_multicoefficient_material_modeling.html.
17. Johnson, P. B. and R. W. Christy, "Optical constants of nobel metals," *Phys. Rev. B*, Vol. 6, 4370–4379, 1972.
18. Veronis, G., S. E. Kocabas, D. A. B. Miller, and S. Fan, "Modeling of plasmonic waveguide components and networks," *J. Comput. Theor. Nanosci.*, Vol. 6, 1808–1826, 2009.
19. Homola, J., S. S. Yee, and G. Gauglitz, "Surface plasmon resonance sensors: Review," *Sensors and Actuators B: Chemical*, Vol. 54, Nos. 1–2, 3–15, Jan. 25, 1999, ISSN 0925-4005, 10.1016/S0925-4005(98)00321-9.
20. Choi, I. and Y. Choi, "Plasmonic Nanosensors: Review and Prospect," *IEEE Journal of Selected Topics in Quantum Electronics*, Vol. 18, No. 3, 1110–1121, May–Jun. 2012.